Peculiar width dependence of the electronic properties of carbon nanoribbons

Motohiko Ezawa
Department of Physics, University of Tokyo, Hongo 7-3-1, 113-0033, Japan
(Received 5 September 2005; revised manuscript received 7 November 2005; published 26 January 2006)

Nanoribbons (nanographite ribbons) are carbon systems analogous to carbon nanotubes. We characterize a wide class of nanoribbons by a set of two integers $\langle p,q\rangle$, and then define the width w in terms of p and q. Electronic properties are explored for this class of nanoribbons. Zigzag (armchair) nanoribbons have similar electronic properties to armchair (zigzag) nanotubes. The band gap structure of nanoribbons exhibits a valley structure with streamlike sequences of metallic or almost metallic nanoribbons. These sequences correspond to equiwidth curves indexed by w. We reveal a peculiar dependence of the electronic property of nanoribbons on the width w.

DOI: 10.1103/PhysRevB.73.045432 PACS number(s): 73.22.−f, 74.78.Na, 78.67.Ch

I. INTRODUCTION

Nanometric carbon materials exhibit various remarkable properties depending on their geometry.[1–11] In particular, intensive research has been made on carbon nanotubes[3] in the last decade. Carbon nanotubes are obtained by wrapping a graphene sheet into a cylinder form. The large interest centers their peculiar electronic properties inherent to quasi-one-dimensional systems.

A similarly fascinating carbon system is a stripe of a graphene sheet named nanographite ribbons, graphene ribbon, or nanographene.[12–19] We call them *carbon nanoribbons* in comparison with carbon nanotubes. They can be manufactured by deposition of nanotubes or diamonds.[20–23] Experimental studies have begun only recently.[24–27] Nanoribbons have a higher variety than nanotubes because of the existence of edges. Wide nanoribbons with zigzag edges have been argued to possess the flat band and show edge ferromagnetism.[15] Though quite attractive materials, their too rich variety has made it difficult to carry out a systematic analysis of carbon nanoribbons.

In this paper we make a proposal to characterize a wide class of nanoribbons by a set of two integers $\langle p,q\rangle$ representing edge shape and width. The width w is defined in terms of p and q. We present a systematic analysis of their electronic property in parallel to that of nanotubes. Carbon nanotubes are regarded as a periodic-boundary-condition problem while carbon nanoribbons are as a fixed-boundary-condition problem. By calculating band gaps they are shown to exhibit a variety of properties in electronic conduction, from metals to typical semiconductors. Several sequences of metallic or almost metallic (MAM) points are found in the valley of semiconducting nanoribbons. We reveal a peculiar dependence of the electronic properties of nanoribbons on the width w. For instance, these sequences and equiwidth curves become almost identical for wide nanoribbons. We also point out that the distribution of van Hove singularities as a function of w shows a peculiar stripe pattern.

This paper is composed as follows. In Sec. II we characterize a wide class of nanoribbons by a set of two integers $\langle p,q\rangle$ and introduce the width w. In Sec. III, making a numerical study, we present an overview of the band gap structure for this class of nanoribbons. In Sec. IV we compare nanoribbons with nanotubes. Zigzag nanoribbons, being indexed by $\langle p,0\rangle$ with even p, correspond to armchair nanotubes; armchair nanoribbons, indexed by $\langle p,1\rangle$ with odd p, correspond to zigzag nanotubes. In Sec. V we discuss sequences of metallic points developed in the valley of semiconducting nanoribbons, where the metallic points on the principal sequence are derived analytically. In Sec. VI we analyze sequences of MAM points more in detail. The nth sequence starts from the metallic armchair nanotube $\langle 3n-1,1\rangle$. It approaches the equiwidth curve with $w=n$ for wide nanoribbons. In Sec. VII we discuss edge effects. We take them into account in three ways: the nonuniform site energy, the nonuniform transfer energy, and the band filling factor.

II. CLASSIFICATION OF CARBON NANORIBBONS

A carbon nanoribbon is a one-dimensional aromatic compound. We have illustrated a typical structure in Fig. 1(a). It consists of carbon atoms of a honeycomb structure. A carbon on the edge is terminated by a different atom such as a hydrogen so that it has no dangling bond. All carbon atoms are connected by σ bonds between sp^2 hybridized orbitals of $2s$, $2p_x$, and $2p_y$, providing with a framework of honeycomb lattice. On the other hand, the π bond is formed between two $2p_z$ orbitals. The π bands cross the Fermi energy, while the σ bands are far away from it. Hence it is a good approximation to take into account only π electrons to investigate electronic properties of nanoribbons. Each carbon atom has the complete shell and there is one electron per atom.

Embedding them into a honeycomb lattice [Fig. 1(b)], we classify nanoribbons as follows. An arbitrary lattice point on a honeycomb lattice is described by the lattice vector

$$\boldsymbol{R} = x\boldsymbol{a} + y\boldsymbol{b}, \tag{1}$$

where $\boldsymbol{a}$ and $\boldsymbol{b}$ are primitive lattice vectors while x and y are integers [Fig. 1(b)]. First we take a basic chain of m connected carbon hexagons, as depicted in dark gray. Second we translate this chain by the translational vector

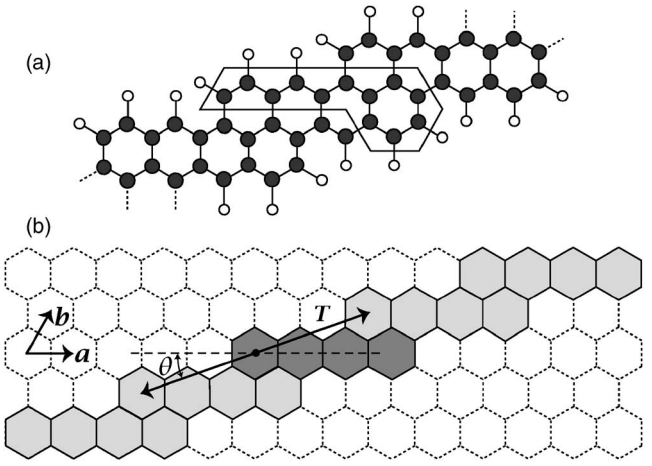

FIG. 1. (a) A typical structure of nanoribbons. A solid circle stands for a carbon atom with one π electron, while an open circle for a different atom such as a hydrogen. A closed area represents a unit cell. It is possible to regard the lattice made of solid circles as a part of a honeycomb lattice. (b) A nanoribbon is constructed from a chain of m connected carbon hexagons, as depicted in dark gray, and by translating this chain by the translational vector $\boldsymbol{T}=\pm q\boldsymbol{a}+\boldsymbol{b}$ many times, as depicted in light gray, where $q<m$. A nanoribbon is indexed by a set of two integers $\langle p,q\rangle$ with $p=m-q$. Here we have taken $m=4$, $q=2$, $p=2$.

$$\boldsymbol{T}=\pm q\boldsymbol{a}+\boldsymbol{b}, \tag{2}$$

as depicted in light gray, where q is an arbitrary integer ($q<m$). Repeating this translation many times we construct a nanoribbon indexed by a set of two integers $\langle p,q\rangle$, where $p=m-q$. In what follows we analyze the class of nanoribbons generated in this way.

The indices p and q specify the type of nanoribbons. The case with $q=0$ represents a zigzag nanoribbon with zigzag edge, while the case with $q=1$ represents an armchair nanoribbon with an armchair edge. The nanoribbons with $\langle 1,0\rangle$, $\langle 1,1\rangle$, and $\langle 2,1\rangle$ are known as polyacene, polyphenanthrene, and polyperynaphthalene,[12,13,20,23,28] respectively [Fig. 2].

We propose to define the width of the nanoribbon by

$$w=2m\sin\theta=\frac{2(p+q)}{\sqrt{3(2q+1)^2+9}}, \tag{3}$$

where θ is the angle between the basic chain and the translational vector

$$\tan\theta=\frac{\sqrt{3}}{2q+1}, \tag{4}$$

as in Fig. 1(b). There is a freedom to normalize the width. We have normalized the width of an armchair nanoribbon indexed by $(p,1)$ to be

$$w=\frac{p+1}{3} \tag{5}$$

by the reason that becomes clear in Sec. VI. Then, the width of zigzag nanoribbons indexed by $(p,0)$ becomes

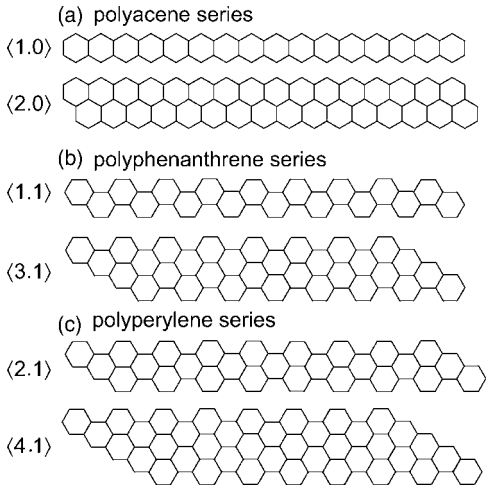

FIG. 2. The geometric configuration of (a) the polyacene series having zigzag edges, (b) the polyphenanthrene series having armchair edges, and (c) the polyperylene series having armchair edges.

$$w=\frac{p}{\sqrt{3}}. \tag{6}$$

The width of a nanoribbon corresponds to the diameter of a nanotube. Though a nanoribbon is specified by two integers, we expect that the electronic properties of wide nanoribbons is mainly controlled by the width w.

The above classification rule is similar to that of nanotubes based on the chiral vector or the rolling up vector,[10,11,29] but it is clearly different since some nanoribbons cannot be rolled up into nanotubes. We discuss the correspondence between nanoribbons and nanotubes in Sec. IV.

III. ELECTRONIC STRUCTURE OF NANORIBBONS

We calculate the band structure of nanoribbons based on the nearest-neighbor tight-binding model, which has been successfully applied to the studies of carbon nanotubes.[10]

The tight-binding Hamiltonian is defined by

$$H=\sum_i \varepsilon_i c_i^\dagger c_i+\sum_{\langle i,j\rangle} t_{ij}c_i^\dagger c_j, \tag{7}$$

where ε_i is the site energy, t_{ij} is the transfer energy, and $c_i^\dagger$ is the creation operator of the π electron at the site i. The summation is taken over the nearest neighbor sites $\langle i,j\rangle$. In the case of nanotubes, constant values are taken for ε_i and t_{ij} due to their homogeneous geometrical configuration. Furthermore, since there exists one electron per one carbon, the band-filling factor is 1/2. In the case of nanoribbons, on the contrary, they would be modified by the existence of the edges. (a) The site energy would be modified by the difference of electronegativity of X, where X represents a different atom such as hydrogen. (b) The transfer energy would be modified by a possible lattice distortion near the edge. (c) The band-filling factor would be modified due to the dipole moment of C-X bonds. It is our basic assumption that the carbon nanoribbon can be analyzed based on this Hamiltonian together with these three modifications.

It is convenient to take a unit cell as shown in Fig. 1(a). There are $(4q+2p+2)$ carbon atoms in a unit cell of the nanoribbon indexed by $\langle p,q\rangle$, as implied that the proper functions of the Hamiltonian H consist of $(4q+2p+2)$ Bloch wave functions $|\psi_i\rangle$. We take overlap integrals as

$$\langle\psi_j|\psi_i\rangle = \delta_{ij}, \tag{8}$$

where δ_{ij} is Kronecker's δ. The π bands of nanoribbon are derived from the Hamiltonian $H(k;p,q)$ with k the crystal momentum, which is a $(4q+2p+2)\times(4q+2p+2)$ matrix. The band structure is determined by

$$\det[\varepsilon I - H(k;p,q)] = 0, \tag{9}$$

where I is a unit matrix due to the overlap integral.

Though the nanoribbon may have different values of ε_i and t_{ij} for atoms on the edge from the others, as we have remarked, the difference is expected to be quite small. We first neglect the difference. Namely, we take the transfer energy to be t between all the nearest neighbor sites and otherwise to be 0. It is generally taken[10] as $t=-3.033$ eV. We also neglect the site energy term in the Hamiltonian (7) by taking all the site energy ε_i equal. We discuss how the gap structure is modified by edge corrections in Sec. VII.

We have solved the eigenvalue problem (9) numerically for ε. Typical band structures are shown in Fig. 3. As is seen in the figures, band structures depend strongly on the parity of q, but only weakly on p. We also find the following: (a) For metallic nanoribbons, the Fermi point of even q is at $k=\pi$, and that of odd q is at $k=0$. (b) For semiconducting nanoribbons, the band gap minimum of even q is at $k=\pi$, and that of odd q is at $k=0$.

As a main result we display an overview of the band gap structure of nanoribbons in Fig. 4. Gapless states (represented by black squares) are metallic, and gapfull states (represented by all other squares) are semiconducting. There are a variety of semiconducting nanoribbons from almost gapless ones (represented by dark gray squares) to large gapfull ones (represented by light gray squares). We observe clearly three emergence patterns of metallic points: (a) Metallic points $\langle p,0\rangle$ for all p. (b) Metallic points $\langle p,1\rangle$ with $p=2,5,8,11,\ldots$. (c) Several sequences of metallic points on "streams" in valleys. We discuss (a) and (b) in Sec. IV, and (c) in Sec. V and VI.

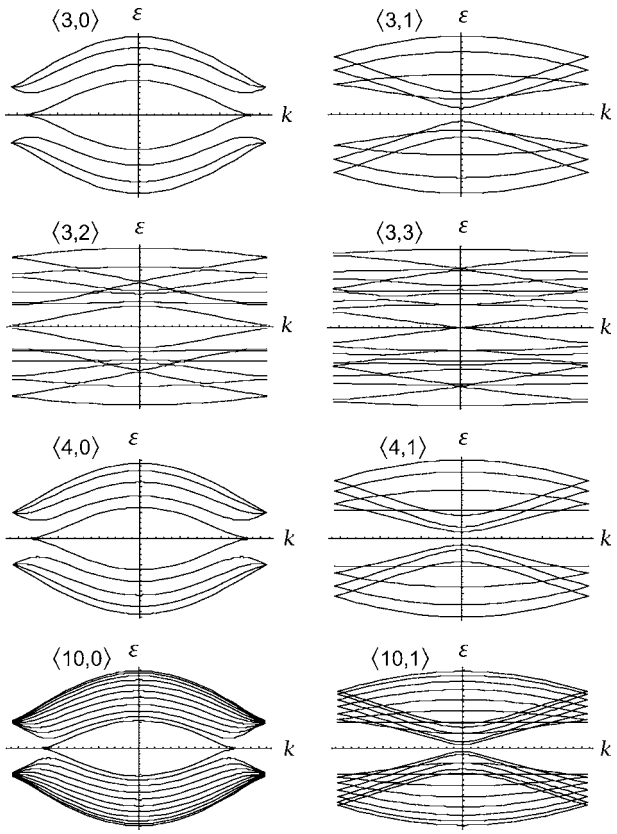

FIG. 3. The band structure of nanoribbons. The horizontal axis is the crystal momentum k, $-\pi<k\leqslant\pi$, while the vertical axis is the energy ε, $-3|t|\leqslant\varepsilon\leqslant 3|t|$ with $|t|=3.033$ eV. The band structure depends strongly on the index q for fixed p, but depends on the index p only weakly for fixed q.

IV. NANORIBBONS VERSUS NANOTUBES

It is observed that nanoribbons indexed by $\langle p,0\rangle$ are metallic for all p, which are in the polyacene series with zigzag edges [Fig. 2(a)]. Nanoribbons indexed by $\langle p,1\rangle$ with $p=2,5,8,11,\ldots$ are found to be also metallic, which have armchair edges [Figs. 2(b) and 2(c)]. This series has period 3, as is a reminiscence of the classification rules familiar for nanotubes. The classification rule says that a nanotube is metallic when n_1-n_2 is an integer multiple of 3, and otherwise semiconducting, where (n_1,n_2) is a chiral vector of the nanotube.

Let us explore the correspondences more in detail. There is a group of nanoribbons each of which is constructed as a development of a nanotube by cutting it along the translational vector. For example, a zigzag nanoribbon $(q=0)$ with even p may be regarded as a development of the armchair nanotube whose chiral vector is $(p/2,p/2)$. All zigzag nanoribbons are metallic, as corresponds to the fact that all armchair nanotubes are metallic. As another example, an armchair nanoribbon $(q=1)$ with odd p may be regarded as a development of a zigzag nanotube whose chiral vector is $[(p+1)/2,0]$. Armchair nanoribbons are metallic with period of 3, as corresponds to the fact that metallic zigzag nanotubes emerge by period of 3.

The correspondence between these metallic points may be explained by the absence of spiral currents in carbon nanotubes. Namely, currents flowing along the axis of nanotubes are not affected by cutting along the axis. There is no direct correspondence between chiral nanotubes and nanoribbons for $q\geqslant 2$.

V. SEQUENCE OF METALLIC NANORIBBONS

It is remarkable that there are series of discrete metallic points on one-dimensional curves in Fig. 4. These curves look like streams in valleys. The prominent ones are at $\langle 1,0\rangle$, $\langle 2,1\rangle$, $\langle 3,3\rangle$, $\langle 4,6\rangle$, $\langle 5,10\rangle$, $\langle 6,15\rangle$, ….We regard them to form the principal sequence of metallic points of nanoribbons.

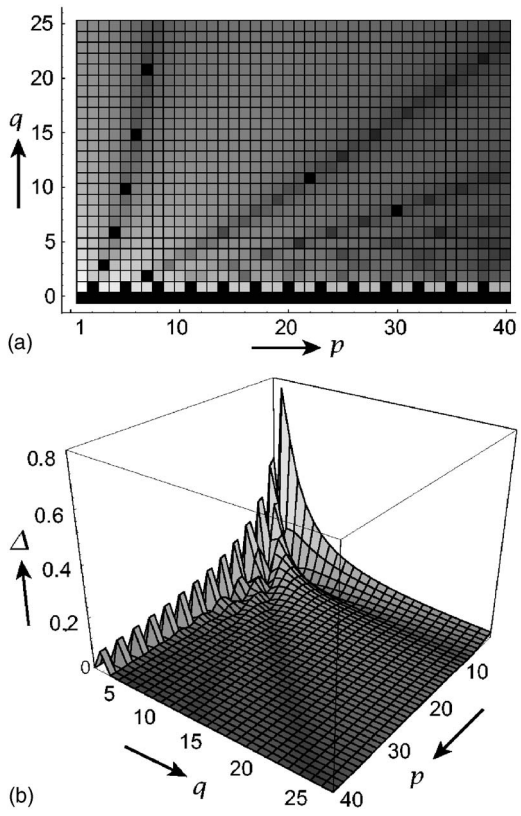

FIG. 4. The band gap structure of nanoribbons. (a) The horizontal and vertical axes represent the indices p and q, respectively. Magnitudes of band gaps are represented by gray squares. Dark (light) gray squares represent small (large) gap semiconductors. Especially, metallic states are represented by black squares. (b) A bird's eye view. The vertical axis is the energy gap Δ in units of $|t|=3.033$ eV. Nanoribbons make a valley structure with stream like sequences of metallic points in the pq plane.

There are also sequences of metallic points on higher curves.

We are able to derive the principal sequence analytically. We start with the observation that the density of states at the Fermi energy is $D(\varepsilon_F)\neq 0$, if the band structure of nanoribbons are gapless; otherwise, $D(\varepsilon_F)=0$. This follows from the reflection symmetry around $\varepsilon=0$ and the existence of one electron per one atom. The reflection symmetry is due to a bipartite lattice structure of graphite.[30] Consequently, to investigate the metallic points, it is enough to analyze

$$\det[H(k;p,q)]=0. \tag{10}$$

We have $D(\varepsilon_F)\neq 0$ if this equation has a solution, and the nanoribbon is gapless; otherwise it is gapfull. We find simple structures at $q=0$ and for $q\geqslant p-1$.

At $q=0$, the determinant (10) is explicitly calculated as

$$\det[H(k;p,0)]=(-1)^{p+1}t^{2p+2}\left(2\cos\frac{k}{2}\right)^{2p+2}. \tag{11}$$

It vanishes for any p at $k=\pi$. Because of this, every zigzag nanoribbon is metallic. It follows that

$$\lim_{p\to\infty}\det[H(k;p,0)]\begin{cases}=0, & \dfrac{2\pi}{3}<|k|\leqslant\pi\\ \neq 0, & |k|\leqslant\dfrac{2\pi}{3}.\end{cases} \tag{12}$$

We have thus verified analytically that the flat band emerges for $2\pi/3<|k|\leqslant\pi$ when the width of nanoribbons is wide enough, as confirms a previous numerical result,[15] where the flat band has been argued to lead to edge ferromagnetism.

For $q=1$ and $p=3n-1$ with integer n, the determinant (10) has a factor such that

$$\det[H(k;p,0)]\propto\sin^2\frac{k}{2}, \tag{13}$$

and the nanoribbon is found to be gapless at $k=0$.

For $q\geqslant p-1$, the determinant (10) is calculated as

$$\begin{aligned}&t^{-(4q+2p+2)}(-1)^{p+1}\det[H(k;p,q)]\\&\quad=p(p+1)\cos 2k+(-1)^q(p^2+p+2)(p+q+1)\cos k\\&\qquad+(p+q+1)^2+\frac{p^2(p+1)^2}{4}+1.\end{aligned} \tag{14}$$

We can prove that $\det[H(k;p,q)]=0$ for a certain k provided that

$$q=\frac{p(p-1)}{2}. \tag{15}$$

Nanoribbons are metallic on the points $\langle p,q\rangle$ with integers p and q with (15). They constitute the principal sequence of metallic points.

It is hard to solve $\det[H(k;p,q)]=0$ analytically for $q<p-1$, though the existence of solutions is clear by numerical analysis as in Fig. 4(a). In this figure there are only three metallic points; the two points are $\langle 7,2\rangle$ and $\langle 22,11\rangle$ on the second sequence, and the last point is $\langle 30,8\rangle$ on the third sequence.

Metallic points on higher sequences are quite curious in this respect. We cannot tell how they arise systematically. However, it may be useless to make efforts to distinguish between metallic and tiny-gap semiconductors too seriously, since the simple tight-binding model we have used will not be accurate enough to predict completely vanishing band gaps. Nevertheless the valley structure with several "streams" will be a significant feature. Hence it is more interesting how the sequences made of MAM (metallic or almost metallic) points are located in valleys.

VI. WIDTH DEPENDENCE OF NANORIBBONS

We have defined the width w of a nanoribbon by the formula (3). We now argue that the sequences of MAM points are indexed by this width.

First, in Fig. 5 we have depicted the band gap as a function of the width w for each fixed value of q. The band gap behaves inversely to w. This reminds us that the band gap of a carbon nanotube is an inverse proportion to the radius. The characteristic feature is that all band gaps with different q

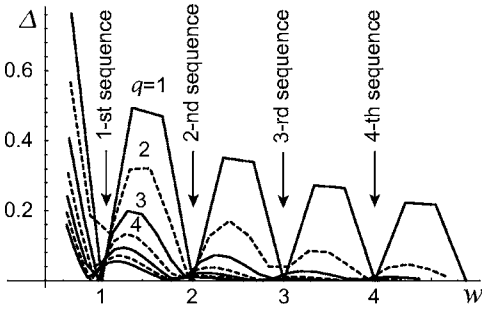

FIG. 5. The band gaps Δ in unit of $|t|=3.033$ eV as a function of the width w. The band gap behaves inversely to w. Band gaps take local minima almost at the same values of the width w for any q.

take local minima almost at the same values of width w, $w=1,2,3,\ldots$. It indicates that nanoribbons with similar width share qualitatively the same electronic properties. The first local minimum corresponds to the principal sequence, which may be regarded as an extension of the armchair nanoribbon indexed by $\langle 2,1\rangle$. In the same way the nth sequence may be regarded as an extension of the armchair nanoribbon with $\langle 3n-1,1\rangle$.

Solving Eq. (3) for p, we have

$$p=-q+\frac{w}{2}\sqrt{3(2q+1)^2+9}. \tag{16}$$

In Fig. 6 we show the curves described by this equation and the sequences of MAM points. It is observed that the nth sequence is almost tangent to the equiwidth curve with $w=n$ at $q=1$. We are able to associate the sequences with the equiwidth curves in this way. These two curves become almost identical for sufficiently wide nanoribbons. This result may be understood as follows. In the case of a continuous ribbon with no lattice structure, the only parameter is the width and the electronic properties is determined by this parameter. We present another indication that the width w is an interesting parameter. We calculate the density of state of an arbitrary $\langle p,q\rangle$ nanoribbon numerically [Fig. 7]. There are many van Hove singularities just as in nanotubes because

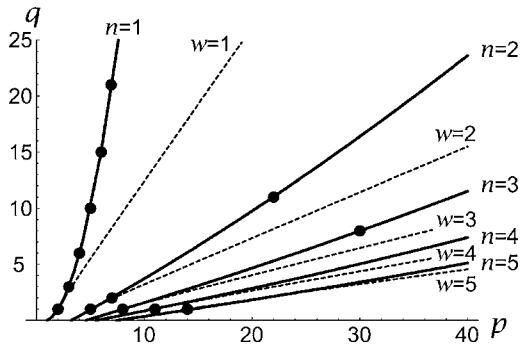

FIG. 6. Illustration of metallic points, sequences, and equiwidth curves. Metallic points are denoted by solid circles. Solid curves represent sequences of MAM points, while dotted curves represent the points $\langle p,q\rangle$ possessing the same width. The nth sequence is tangent to the equiwidth curve with $w=n$ at $q=1$. These two curves become almost identical for sufficiently wide nanoribbons.

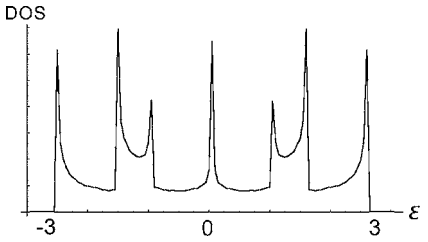

FIG. 7. The density of state (DOS) of the $\langle 1,0\rangle$ nanoribbon. The horizontal axis is the energy ε. There are many van Hove singularities because of one-dimensional structure of nanoribbon.

nanoribbons are also one-dimensional compounds. The global structure of the density of state is determined by van Hove singularities. These peaks can be measured experimentally by Raman scattering.[7,24,31,32]

We calculate the energies ε at which van Hove singularities develop due to the local band flatness at $k=0$ for various $\langle p,q\rangle$ nanoribbons. Note that the optical absorption is dominant at $k=0$ because the dispersion relation $\varepsilon=ck$ with c the light velocity. On the other hand the width w is determined by p and q as in (3). We show the energy ε of this peak as a function of w in Fig. 8. A peculiar stripe pattern is manifest there. In particular, the maximum and minimum values take almost the same values $\pm 3|t|$, reflecting the electronic properties of a graphite.[10] The fact that they are on smooth curves justifies a physical meaning of the width w. This stripe pattern would be accessible experimentally by way of Raman scattering.

VII. EDGE CORRECTIONS

We finally study how the gap structure is modified by the existence of edges in a carbon nanoribbon. All carbon atoms in a carbon nanotube are equivalent in the sense that each of them is always surrounded by three carbon atoms. In contrast, this is not the case for a nanoribbon, where a carbon on the edge has less neighboring carbon atoms. The presence of C-X bonds introduces carbon atoms on edge with a different nature. We assume that the edge effects can be taken into account by modifying the band-filling factor, the transfer energy t_{ij} and the site energy ε_i in the Hamiltonian (7). We take

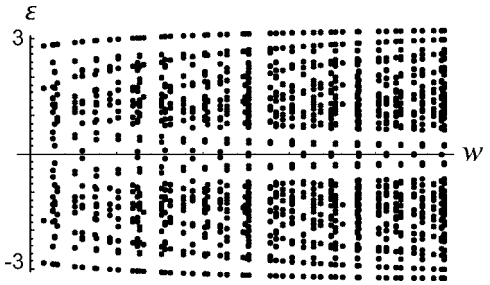

FIG. 8. Plot of van Hove singularities in the w-ε plane. For a given $\langle p,q\rangle$ nanoribbon, we calculate the width w and the energies ε at which van Hove singularities develop. We have plotted the points (w,ε) for $q=1,2,3,4$ and for all p in the region $w\leqslant 3$. A stripe pattern is manifest.

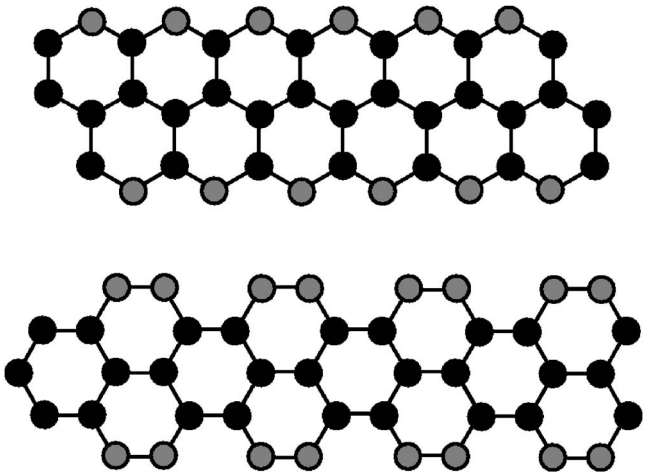

FIG. 9. Illustration of edge carbons and bulk carbons. A gray circle denotes an edge carbon connected by two carbons and a hydrogen. A black circle denotes a bulk carbon connected by three carbons. The energy and the transfer energy associated with edge carbons are set to be $\varepsilon_{\text{edge}}$ and t_{edge}, respectively. Hydrogen atoms are omitted in this figure.

$t_{ij}=t_{\text{edge}}$ and $\varepsilon_i=\varepsilon_{\text{edge}}$ for those associated with edge carbons, and $t_{ij}=t_{\text{bulk}}$ and $\varepsilon_i=\varepsilon_{\text{bulk}}$ for bulk carbons (Fig. 9).

First, the band-filling factor is affected by the dipole moment of C-X bonds. The change of electron numbers is given at most by the number of C-X bonds and is small for wide nanoribbons. This effect does not modify the band structure, but only changes the occupancy of the band. As a result, semiconducting nanoribbons tend to become metallic nanoribbons.

Second, the transfer energy is affected by the change of the distance between two carbons near the edge. The distortion does not break the inversion symmetry of the band structure. Recalculating the band structure of various nanoribbons, we have found that the difference is hardly recognizable. We show the band structure of the $\langle 5,0\rangle$ nanoribbon in Fig. 10, assuming a large correction such that $t_{\text{edge}}=0.7t_{\text{bulk}}$ to make the difference recognizable.

Finally, the site energy is affected by the difference of electronegativity of X. The effect is expected to be also very small because the site energy of π electrons is mainly determined by carbon atoms. It breaks the inversion symmetry because the lattice of carbon atoms cannot be resolved into two sublattices any more.[30] For this reason the Fermi energy is moved from $\varepsilon_{\text{bulk}}=0$. The recalculated band structure of zigzag and armchair nanoribbons is given by assuming a large choice of the edge correction, $\varepsilon_{\text{edge}}=\varepsilon_{\text{bulk}}+0.3t$, in

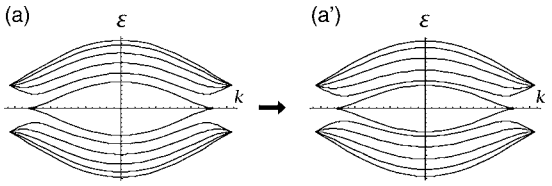

FIG. 10. (a) The original band structure of the $\langle 5,0\rangle$ nanoribbon. (a′) The band structure of the nanoribbon with the choice of $t_{\text{edge}}=0.7t_{\text{bulk}}$. The difference is hardly recognizable.

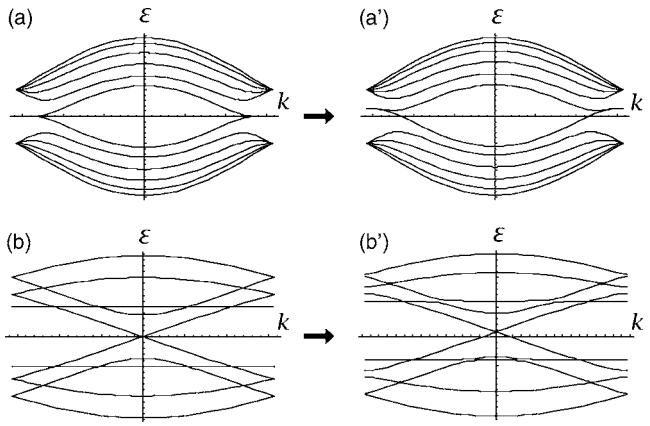

FIG. 11. (a) and (b) The original band structures of the $\langle 5,0\rangle$ and $\langle 2,1\rangle$ nanoribbons. (a′) and (b′) The band structures of the nanoribbon with the choice of $\varepsilon_{\text{edge}}=\varepsilon_{\text{bulk}}+0.3t$. The inversion symmetry is broken and the Fermi energy is slightly moved from $\varepsilon_{\text{bulk}}=0$.

Fig. 11. The modification is small as expected, though some of metallic armchair nanoribbons become semiconducting.

In general the transfer-energy correction must be smaller than the site-energy correction because the former is due to a structural distortion while the latter is due to the electronegativity. The transfer-energy correction will be negative by considering the expansion effect near the surface. On the other hand, the site-energy correction will be positive or negative if the relative electronegativity of the edge atoms is positive or negative.

We present an overview of the band gap structure of various $\langle p,q\rangle$ nanoribbons with the edge corrections by making a choice of $\varepsilon_{\text{edge}}=\varepsilon_{\text{bulk}}+0.05t$ and $t_{\text{edge}}=0.99t_{\text{bulk}}$ in Fig. 12; and by making a choice of $\varepsilon_{\text{edge}}=\varepsilon_{\text{bulk}}+0.10t$ and $t_{\text{edge}}=0.95t_{\text{bulk}}$ in Fig. 13. Comparing them with Fig. 4, some features of edge effects are manifest: (a) The valley structure with streamlike sequences remains as they are. (b) All zigzag nanoribbons remains gapless. (c) Armchair nanoribbons are most strongly affected. (d) Edge effects are negligible for wide nanoribbons.

VIII. DISCUSSION

We have systematically studied and presented a gross view of the electronic properties for a wide class of carbon nanoribbons. They exhibit a rich variety of band gaps, from metals to typical semiconductors. Zigzag and armchair nanoribbons have electronic properties similar to nanotubes, but other nanoribbons are quite different. It is remarkable that there exist sequences of metallic or almost metallic nanoribbons which look like streams in valleys made of semiconductors. They approach equiwidth curves for wide nanoribbons. We have revealed a peculiar dependence of the electronic properties of nanoribbons on the width w. These characteristic features are not affected strongly by edge corrections even for narrow nanoribbons.

In our analysis we have employed the nearest-neighbor tight-binding model. It is worthwhile to calculate band gaps by more rigorous methods such as a density-functional

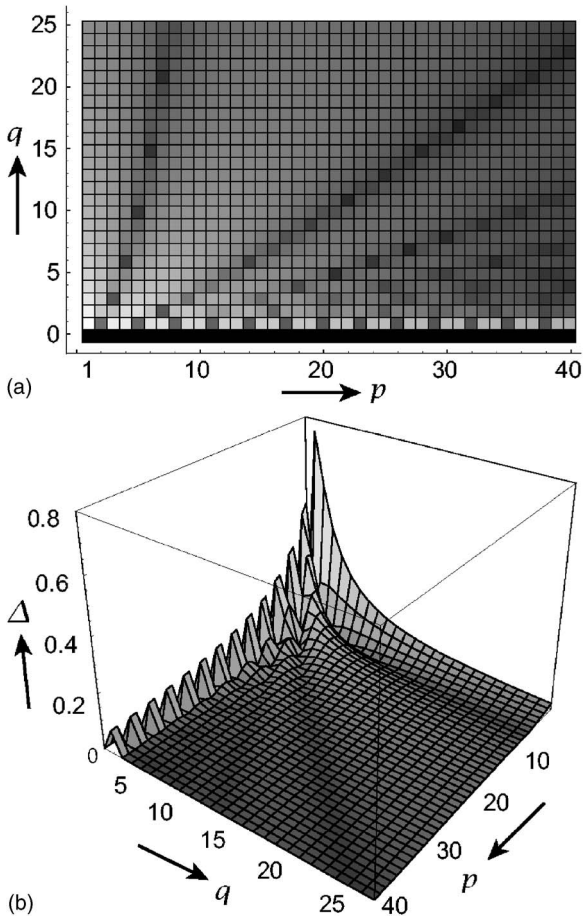

FIG. 12. The band gap structure of nanoribbons with the edge correction $\varepsilon_{\text{edge}}=\varepsilon_{\text{bulk}}+0.05t$ and $t_{\text{edge}}=0.99t_{\text{bulk}}$. See Fig. 4 for other details. Nanoribbons make a valley structure with streamlike sequences of almost metallic points in the pq plane. Zigzag nanoribbons remain gapless. Armchair nanoribbons are most strongly affected by edge corrections.

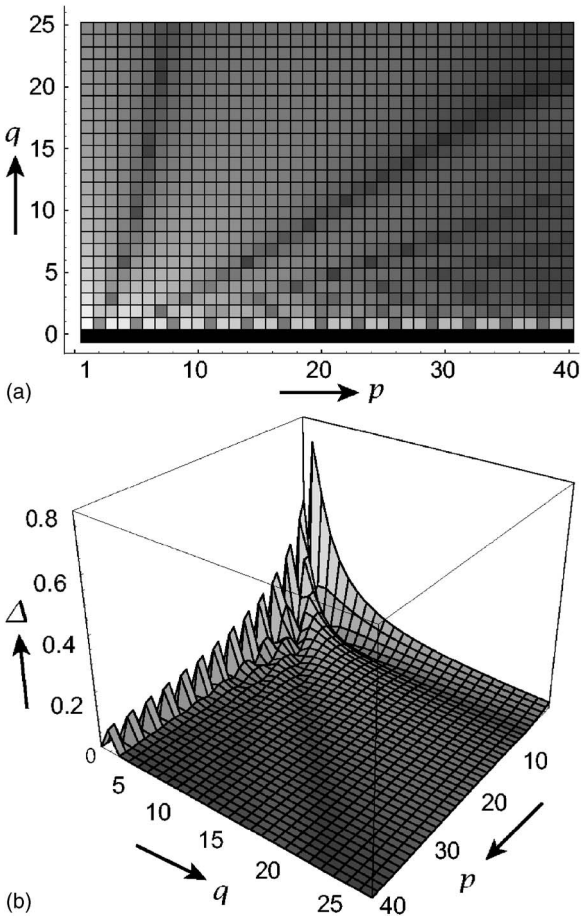

FIG. 13. The band gap structure of nanoribbons with the edge correction $\varepsilon_{\text{edge}}=\varepsilon_{\text{bulk}}+0.10t$ and $t_{\text{edge}}=0.95t_{\text{bulk}}$. See Fig. 4 for other details. Nanoribbons make a valley structure with streamlike sequences of almost metallic points in the pq plane. Zigzag nanoribbons remain gapless. Armchair nanoribbons are most strongly affected by edge corrections.

theory.[33–36] It is interesting to examine whether metallic points on the sequences we have discovered remain gapless in these calculations. We also note that edge corrections have been calculated by a tight-binding density-functional method in several cases for other materials.[37–41] Needless to say it is an extremely hard task to carry out these calculations and practically impossible to make a systematic analysis based on them. Our results on the electronic property of carbon nanoribbons will be useful as a guidepost for those advanced studies.

In passing, we remark that experimental studies of nanoribbons are just in the beginning stage[24–26] in comparison with the study of nanotubes. This may be due to a difficulty of manufacturing and selecting good samples, but the recent technical developing will soon solve this problem. The band gap study of various nanoribbons presented in this paper may be a basic step for various application of carbon nanoribbons.

ACKNOWLEDGMENTS

The author is very thankful to Professors H. Aoki and R. Saito for various stimulating discussions.

[1] M. S. Dresselhaus, G. Dresselhaus, K. Sugihara, I. L. Spain, and H. A. Goldberg, *Graphite Fibers and Filaments*, Springer Series in Material Science Vol. 5 (Springer-Verlag, Berlin, 1988).

[2] H. W. Kroto, J. R. Heath, S. C. O'Brien, R. F. Curl, and R. E. Smalley, Nature (London) **318**, 167 (1985).

[3] S. Iijima, Nature (London) **354**, 56 (1991).

[4] N. Hamada, S. I. Sawada, and A. Oshiyama, Phys. Rev. Lett. **68**, 1579 (1992).

[5] R. Saito, M. Fujita, G. Dresselhaus, and M. S. Dresselhaus, Appl. Phys. Lett. **60**, 18 (1992).

[6] J. W. Mintmire, B. I. Dunlap, and C. T. White, Phys. Rev. Lett. **68**, 631 (1992).
[7] A. Jorio, R. Saito, J. H. Hafner, C. M. Lieber, M. Hunter, T. McClure, G. Dresselhaus, and M. S. Dresselhaus, Phys. Rev. Lett. **86**, 1118 (2001).
[8] N. Shima and H. Aoki, Phys. Rev. Lett. **71**, 4389 (1993).
[9] J. W. G. Wildöer, L. C. Venema, A. G. Rinzler, R. E. Smalley, and C. Dekker, Nature (London) **391**, 59 (1998).
[10] R. Saito, G. Dresselhaus, and M. S. Dresselhaus, *Physical Properties of Carbon Nanotubes* (Imperial College Press, London, 1998).
[11] M. Ouyang, J. L. Huang, and C. M. Lieber, Annu. Rev. Phys. Chem. **53**, 201 (2002).
[12] S. Kivelson and O. L. Chapman, Phys. Rev. B **28**, 7236 (1983).
[13] K. Tanaka, K. Ohzeki, S. Nankai, T. Yamabe, and H. Shirakawa, J. Phys. Chem. Solids **44**, 1069 (1983).
[14] B. I. Dunlap, Phys. Rev. B **49**, 5643 (1994).
[15] M. Fujita, K. Wakabayashi, K. Nakada, and K. Kusakabe, J. Phys. Soc. Jpn. **65**, 1920 (1996).
[16] K. Wakabayashi, M. Fujita, H. Ajiki, and M. Sigrist, Phys. Rev. B **59**, 8271 (1999).
[17] K. Wakabayashi and M. Sigrist, Phys. Rev. Lett. **84**, 3390 (2000).
[18] S. Ryu and Y. Hatsugai, Phys. Rev. B **67**, 165410 (2003).
[19] E. J. Duplock, M. Scheffler, and P. J. D. Lindan, Phys. Rev. Lett. **92**, 225502 (2004).
[20] M. Murakami, S. Iijima, and S. Yoshimura, J. Appl. Phys. **60**, 3856 (1986).
[21] M. Zhang, D. H. Wu, C. L. Xu, and W. K. Wang, Nanostruct. Mater. **10**, 1145 (1998).
[22] Y. Shibayama, H. Sato, T. Enoki, and M. Endo, Phys. Rev. Lett. **84**, 1744 (2000).
[23] A. M. Affoune, B. L. V. Prasad, H. Sato, T. Enoki, Y. Kaburagi, and Y. Hishoyama, Chem. Phys. Lett. **348**, 17 (2001).
[24] L. G. Cancado, M. A. Pimenta, B. R. A. Neves, G. Medeiros-Ribeiro, T. Enoki, Y. Kobayashi, K. Takai, K. I. Fukui, M. S. Dresselhaus, R. Saito, and A. Jorio, Phys. Rev. Lett. **93**, 047403 (2004).
[25] Y. Niimi, T. Matsui, H. Kambara, K. Tagami, M. Tsukada, and H. Fukuyama, Appl. Surf. Sci. **241**, 43 (2005).
[26] Y. Kobayashi, K. I. Fukui, T. Enoki, K. Kusakabe, and Y. Kaburagi, Phys. Rev. B **71**, 193406 (2005).
[27] T. Matsui, H. Kambara, Y. Niimi, K. Tagami, M. Tsukada, and H. Fukuyama, Phys. Rev. Lett. **94**, 226403 (2005).
[28] M. Yudasaka, Y. Tasaka, M. Tanaka, H. Kamo, Y. Ohki, S. Usami, and S. Yoshimura, Appl. Phys. Lett. **64**, 3237 (1994).
[29] G. Seifert, H. Terrones, M. Terrones, G. Jungnickel, and Th. Frauenheim, Phys. Rev. Lett. **85**, 146 (2000).
[30] E. H. Lieb, Phys. Rev. Lett. **62**, 1201 (1989).
[31] A. M. Rao, A. Jorio, M. A. Pimenta, M. S. S. Dantas, R. Saito, G. Dresselhaus, and M. S. Dresselhaus, Phys. Rev. Lett. **84**, 1820 (2000).
[32] P. Kim, T. W. Odom, J.-L. Huang, and C. M. Lieber, Phys. Rev. Lett. **82**, 1225 (1999).
[33] D. Porezag, Th. Frauenheim, Th. Köhler, G. Seifert, and R. Kaschner, Phys. Rev. B **51**, 12947 (1995).
[34] K. Kusakabe and M. Maruyama, Phys. Rev. B **67**, 092406 (2003).
[35] M. Maruyama, K. Kusakabe, S. Tsuneyuki, K. Akagi, Y. Yoshimoto, and J. Yamauchi, J. Phys. Chem. Solids **65**, 119 (2004).
[36] Y. Higuchi, K. Kusakabe, N. Suzuki, S. Tsuneyuki, J. Yamauchi, K. Akagi, and Y. Yoshimoto, J. Phys.: Condens. Matter **16**, S5689 (2004).
[37] G. Seifert, Th. Frauenheim, T. Köhler *et al.*, Phys. Status Solidi B **225**, 393 (2001).
[38] Th. Köhler, Th. Frauenheim, Z. Hajnal, and G. Seifert, Phys. Rev. B **69**, 193403 (2004).
[39] S. M. Lee, M. A. Belkhir, X. Y. Zhu, Y. H. Lee, Y. G. Hwang, and Th. Frauenheim, Phys. Rev. B **61**, 16033 (2000).
[40] Z. Hajnal, G. Vogg, L. J.-P. Meyer, B. Szücs, M. S. Brandt, and Th. Frauenheim, Phys. Rev. B **64**, 033311 (2001).
[41] G. Seifert, T. Köhler, H. M. Urbassek, E. Hernández, and Th. Frauenheim, Phys. Rev. B **63**, 193409 (2001).